2-Hydroxypyridine ↔ 2-Pyridone Tautomerization: Catalytic Influence of Formic Acid

Montu K. Hazra[†] **and Tapas Chakraborty***[,†,‡]

Department of Chemistry, Indian Institute of Technology, Kanpur, UP 208016, India, and Department of Physical Chemistry, Indian Association for the Cultivation of Science, Jadavpur, Calcutta 700032, India

Received: February 1, 2006; In Final Form: April 17, 2006

A 1:1 hydrogen-bonded complex between 2-pyridone and formic acid has been characterized using laser-induced-fluorescence excitation and dispersed fluorescence spectroscopy in a supersonic jet expansion. Under the same expansion condition, the fluorescence signal of the tautomeric form of the complex (2-hydroxypyridine···formic acid) is absent, although both the bare tautomeric molecules exhibit well-resolved laser-induced-fluorescence spectra. Quantum chemistry calculation at the DFT/B3LYP/6-311++G** level predicts that in the ground electronic state the activation barrier for tautomerization from hydroxy to keto form in bare molecules is very large (∼34 kcal/mol). However, the process turns out to be nearly barrierless when assisted by formic acid, and double proton transfer occurs via a concerted mechanism.

1. Introduction

Tautomerization reactions involving double proton transfer are ubiquitous in chemical and biological processes.[1−7] In biology, tautomeric transformation of the purine and pyrimidine bases results in mispairing between the complementary bases in a double-stranded DNA molecule, and this has been considered to be responsible for point mutation.[2] To understand the details of such a tautomerization reaction in a complex natural system, a lot of attention has been paid in recent years to a number of suitable model molecules. The 2-hydroxypyridine (2HP) ↔ 2-pyridone (2PY) tautomeric pair is such a convenient model, and it may mimic the tautomerization of the uracil and thymine bases. The system has been investigated by several groups using various spectroscopic and theoretical methods.[8−22] In this paper, we report our experimental and theoretical studies of the catalytic effect of formic acid (FA) on tautomerization of this important model system in the gas phase.

Recently, Hamaguchi et al.[23] have investigated the catalytic effect of acetic acid (AA) on the 2-aminopyridine (2AP) ↔ 2(1*H*)-pyridinimine (1H2PI) tautomeric equilibrium. Both tautomeric forms are found to be present in a hexane solution at room temperature. The emission spectrum of the hydrogen-bonded complex of the imine tautomer shows a very large red shift compared to the amine form; the emission maximum of the former appears at 480 nm and the excited state lifetime is 3.2 ns. On the basis of the measured data, the authors concluded that tautomerization in the complex occurs via stepwise transfer of the two protons within 5 ps in the excited state. A theoretical study of this acid catalyzed tautomerization process has been reported by Hung et al.[24] The CIS/6-31+G(d′,p′) level of calculation predicts that 2AP···AA → 1H2PI···AA conversion via double proton transfer involves two transition state configurations corresponding to a two-step process. However, to our knowledge, no gas-phase experiment on this system has been reported.

For the present system, although the existence of both tautomeric forms (2HP and 2PY) in the ground electronic state has been verified earlier using rotational, vibrational, and electronic spectroscopies,[25−28] to our knowledge an experimental investigation about the catalytic effect of carboxylic acids on the tautomeric equilibrium has not been initiated, although a quantum chemistry prediction for the process has been attempted.[29] The results of the earlier studies indicate that bare 2HP is more stable than 2PY, and the barrier for tautomeric conversion in the gas phase is quite high (∼40 kcal/mol, depending on employed methods and basis sets).[30−35] In the present study, we have attempted to characterize the formic acid complexes of the tautomeric pair (2HP···FA and 2PY···FA) using laser-induced-fluorescence excitation and dispersed fluorescence spectroscopy. The energetic and geometric parameters of the two complexes and the potential energy surface for 2HP···FA ↔ 2PY···FA tautomeric conversion have been investigated using density functional theory (DFT) method.

2. Methods

2.1. Experiment. The experimental setup to measure the fluorescence excitation and dispersed fluorescence spectra has been described before.[36] Briefly, the carrier gas helium at a pressure of 2 atm was passed successively through a cell containing formic acid at 0 °C and a second glass cell containing 2HP at 100 °C, and the final gas mixture was expanded into vacuum through a pulsed nozzle (General Valve) of orifice diameter 0.5 mm. The expansion-generated clusters were excited by the frequency-doubled output of a tunable dye laser (Sirah and Plasma Technik, Model Cobra Stretch), which was pumped by the second harmonic (λ = 532 nm) of a Nd:YAG laser (Spectra Physics, Model INDI). The laser beam (line width ∼ 0.5 cm^{-1}) intersects the free jet perpendicularly at about 12 mm downstream of the nozzle orifice, and the emission is collected from the intersection point in a direction perpendicular to both the laser and the free jet. Fluorescence excitation spectra were measured by detecting the total fluorescence by a Hamamatsu R928 photomultiplier tube (PMT). The output signals of the PMT were processed by a boxcar averager (Model RS250, Stanford Research Corp.). The averaged output of the boxcar was stored in a computer using a home-built data acquisition

* To whom correspondence should be addressed. Phone: (91) (33) 2473 4971. Fax: (91) (33) 2473 2805. E-mail: pctc@iacs.res.in.
† Indian Institute of Technology.
‡ Indian Association for the Cultivation of Science.

10.1021/jp060687v CCC: $33.50
Published on Web 06/30/2006

system. To measure the dispersed fluorescence spectra, we have used a 0.75 m monochromator (Spex, Model 750 M) having a grating of groove density 2400/mm and a double staged Peltier cooled ICCD (Jovin Yvon, Model 3000V) detector.

2.2. Theory. The geometries of 2HP and 2PY, their 1:1 complexes with FA, and the transition states (TS) connecting the respective tautomeric pairs were calculated at the DFT/B3LYP/6-31G** level and also by ab initio method at the MP2/6-31G** level. The Gaussian 03 suite of programs was used to perform all calculations.[37] Since the intermolecular distances and the energy barrier for tautomeric transformation are quite sensitive to the size of the basis set, the DFT predicted geometries were further optimized using a higher basis set (6-311++G**). The TS connecting 2HP ↔ 2PY and 2HP···FA ↔ 2PY···FA tautomeric pairs have been located using the synchronous transit-guided quasi-Newton (STQN) method.[38] Normal-mode vibrational analysis was performed to verify that the optimized geometries of all the normal molecular species have only positive frequencies, and a TS species has only one imaginary frequency. The normal-mode frequencies were also used to find the effect of a zero point energy correction on tautomerization barrier heights. Basis set superposition errors in the calculated binding energies (E_{HB}) of the two complexes are corrected by the counterpoise (CP) method of Boys and Bernardi.[39] Intrinsic reaction coordinate (IRC) and potential energy surface (PES) calculations were performed at the DFT/B3LYP level using the 6-31G** basis set.

3. Result and Discussion

3.1. Experiment. *3.1.A. Fluorescence Excitation (FE) Spectra.* Our recorded FE spectra of 2HP and 2PY are identical to those reported previously by Nimlos et al.[26] and Matsuda et al.,[40−42] respectively. The $S_1 \leftarrow S_0$ electronic origin bands of the two molecules appear at 36 123 and 29 832 cm^{-1}, respectively. Reference 42 shows that the electronic origin band of 2HP undergoes a red shift of 666 cm^{-1} on formation of a 1:1 complex with water. In contrast, the same effect with 2PY causes a blue shift of 633 cm^{-1}.[40] In the present case, to record the FE spectra of the two complexes, we scanned the excitation frequencies over wide spectral ranges around the two monomer origin bands. We have notice that in the 2PY spectral region the fluorescence signal shows a large enhancement (more than 15 times compared to that of the bare molecule), but under the same expansion condition no new band shows up on scanning the excitation laser wavelength in the 2HP absorption region (272−287 nm). Thus, the absence of any absorption band corresponding to 2HP···FA complex in the FE spectrum indicates that either the species is nonfluorescent or it probably undergoes tautomeric transformation to 2PY···FA during collisional cooling in the supersonic jet expansion in the ground electronic state. Below, we provide DFT predicted energetic and kinetic data in favor of the latter possibility.

The first 800 cm^{-1} of the measured FE spectrum of 2PY···FA is presented in Figure 1. The electronic origin band appears at 31 064 cm^{-1}, and it is 1232 cm^{-1} blue shifted from the 2PY monomer origin ("A" origin).[40] By changing the backing pressures of nozzle expansion as well as the sample concentration in the preexpansion gas mixture, we have verified that the relative intensities of the bands in the spectrum remain practically unchanged. Thus, we conclude that all the vibronic bands in the spectrum belong to the $S_1 \leftarrow S_0$ absorption system of 2PY···FA mixed dimer.

According to ref 40, the prominent vibronic bands within the first 500 cm^{-1} of the FE spectrum of 2PY monomer appear only at 217, 255, and 440 cm^{-1}. In contrast, Figure 1 shows

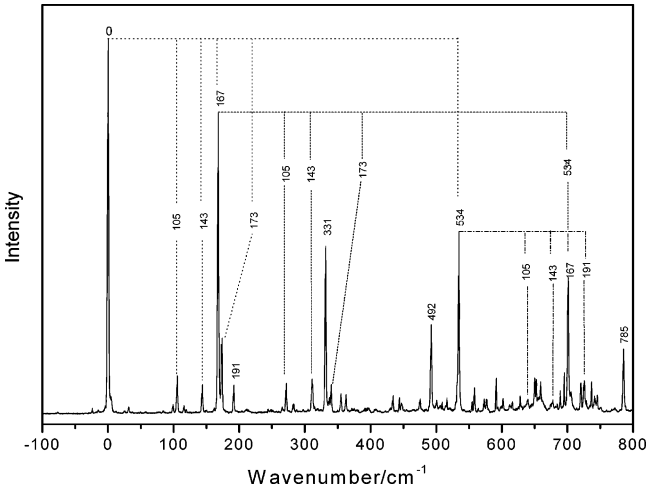

Figure 1. Fluorescence excitation spectrum for $S_1 \leftarrow S_0$ electronic transition of 2PY···FA mixed dimer in a supersonic free jet expansion. The electronic origin band at 31 064 cm^{-1} has been considered as the zero (0) of the frequency (cm^{-1}) scale. Assignments of the major vibronic bands have been discussed in the text.

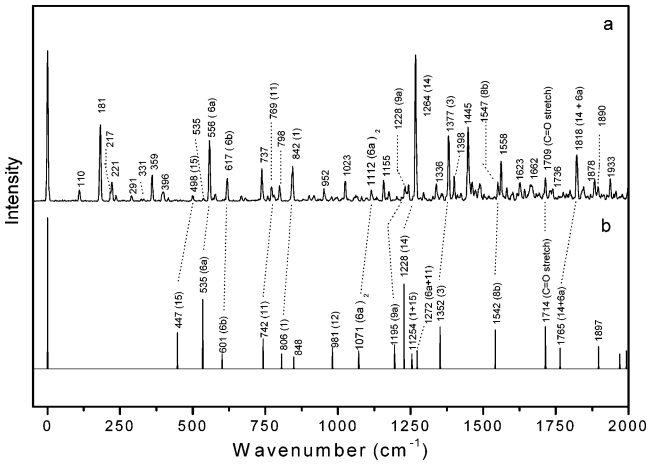

Figure 2. Comparison between the dispersed fluorescence spectrum of 2PY···FA mixed dimer (a) measured by exciting the $S_1 \leftarrow S_0$ origin band and that for 2PY monomer (b) as reported in ref 26. The latter has been reproduced here in stick spectral format.

that there are many low-frequency bands, e.g., at 105, 143, 167, 173, and 191 cm^{-1}. Therefore, these bands can only correspond to the intermolecular hydrogen bond vibrations of the dimer in the excited state. Of these, the 167 cm^{-1} band appears to be the most intense vibronic fundamental and the 331 and 492 cm^{-1} bands can be assigned to its first and second overtones. Again, the band at 534 cm^{-1}, which is likely to represent a transition associated with the aromatic ring, is the second most intense vibronic fundamental in the spectrum and all the low-frequency features on the origin are built off this band as combinations. The detailed assignments of these bands will be discussed elsewhere.

3.1.B. Dispersed Fluorescence (DF) Spectra. The first 2000 cm^{-1} of the DF spectrum measured by exciting the $S_1 \leftarrow S_0$ origin of 2PY···FA is presented in Figure 2a. The same for the 2PY monomer was measured earlier by Nimlos et al.,[26] and the spectrum has been reproduced here (Figure 2b) in stick spectral format to depict the hydrogen bond induced shifts in vibronic spectral frequencies and intensity distortions. The frequencies of the prominent vibronic bands in Figure 2a and their assignments are presented in Table 1. The Varsanyi nomenclature scheme of monosubstituted benzene derivatives[43]

TABLE 1: Vibronic Band Assignments of DF Spectra of 2PY Monomer and 2PY···FA Dimer Measured by Exciting Their $S_1 \leftarrow S_0$ Electronic Origin Bands[a]

2PY		2PY···FA		
observed	predicted	observed	predicted	assignment
0		0		origin
		110	113	in-plane sliding (X_1^0)
		181	180	H-bond stretching (Y_1^0)
		217	221	X_2^0
		221	216	in-plane COOH bending (Z_1^0)
		291		$Y_1^0 + X_1^0$
		331		$Z_1^0 + X_1^0$
		359		Y_2^0
	383	394	394	16a(?)
		398		$X_2^0 + Y_1^0$
447	453	498	494	15
		535		Y_3^0
535	543	556	559	6a
		576		$X_2^0 + Y_2^0$/16a + Y_1^0
601	612	617	633	6b
		666		6a + X_1^0
		737		6a + Y_1^0
742	760[b]	769	766[b]	$16a_2^0$/11(?)/(4 + butterfly)[c]
		777		6a + Z_1^0
		798		6b + Y_1^0
806	810	842	842	1
		915		6a + Y_2^0
		952		1 + X_1^0
		1023		1 + Y_1^0
1071		1112		$6a_2$
		1155	1163	9b
		1173		6a + 6b
		1201		1 + Y_2^0
1195	1210	1228	1236	9a/$6b_2^0$
		1239		11 + X_1^0 + Y_2^0
1228	1226	1264	1261	14
		1293		$6a_2$ + Y_1^0
		1336		9b + Y_1^0/9a + X_1^0
1352	1374	1377	1386	3/14 + X_1^0
		1398		1 + 6a
		1445		14 + Y_1^0
		1458		1 + 6b
1542	1564	1547	1568	8b
		1558		3 + Y_1^0
		1623		14 + Y_2^0
		1658		14 + 16a
		1662		14 + X_2^0 + Y_1^0
1714	1729	1709	1683	C═O stretch
		1726		8b + Y_1^0
		1736		3 + Y_2^0
1765		1818		14 + 6a/C═O stretch + X_1^0
		1878		14 + 6b
		1890		C═O stretch + Y_1^0
		1933		6a + 3

[a] A scaling factor of 0.99 has been used on theoretically predicted (B3LYP/6-311++G**) frequencies to match the observed band positions. [b] Predicted frequency for 11 mode. [c] In the case of 2-PY···FA complex, the predicted frequencies for 4 and butterfly modes are 723 and 46 cm^{-1}, respectively.

has been used to denote the vibronic fundamentals of both the 2PY monomer and 2PY···FA complex. The vibronic assignments have been aided by the predicted frequencies at the B3LYP/6-311++G** level of calculation.

The first prominent band in the DF spectrum of 2PY monomer (Figure 2b) appears at 447 cm^{-1}, whereas the spectrum of the dimer (Figure 2a) shows many distinct bands below this frequency. Therefore, we assign these low-frequency bands to the intermolecular hydrogen bond vibrations. Visualization of the atomic displacement pattern of the six calculated intermolecular vibrations (see Supporting Information, Figure 1), reveals that the lowest frequency band at 110 cm^{-1} can be assigned to the in-plane sliding vibration at the hydrogen-bonded interface. The next strong band at 181 cm^{-1} can be assigned as the hydrogen bond stretching fundamental, which is in excellent agreement with the calculated frequency of 180.0 cm^{-1}. The peak at 221 cm^{-1} is assigned to the fundamental of the in-plane −COOH bending based on a calculated frequency of 216.0 cm^{-1}, and a shoulder of this band at 217 cm^{-1} has been assigned to the overtone of the 110 cm^{-1} vibronic fundamental. Although calculation predicts that the torsional frequency of the hydrogen-bonded interface is 221 cm^{-1}, the fundamental for this mode

TABLE 2: Theoretically Predicted Relative Energies[a] (kcal/mol) of 2PY and 2PY···FA Complex in Comparison to 2HP and 2HP···FA, Respectively, As Predicted by Different Levels of Theoretical Calculation

level of calculation	$\Delta E_{2PY-2HP}$	$\Delta E_{2PY\cdots FA-2HP\cdots FA}$
MP2/6-31G**	2.27 (2.20)[b]	−0.31
MP2/6-311++G**	2.82 (2.82)[c]	0.50
B3LYP/6-31G**	−0.01 (0.03)[b]	−2.33
B3LYP/6-311++G**	−0.88 (−0.86)[c]	−3.04
BH-LYP/6-311++(2d,2p)	0.99 (1.00)[c]	−2.00

[a] Negative values of relative energies indicate that 2PY or 2PY···FA is more stable than 2HP or 2HP···FA complex. [b] From ref 31. [c] From ref 30.

should be absent in the DF spectrum because of symmetry restriction. The assignments of the other bands are presented in Table 1. In ref 26, Nimlos et al. did not offer any assignment of the vibronic bands in the DF spectrum of 2PY. Here, we suggest assignments of the monomer bands, and the one-to-one correspondences between the monomer and dimer transitions are indicated by dotted lines.

The vibronic bands at 556, 617, 842, 1264, and 1377 cm^{-1} in Figure 2a have been assigned to different in-plane fundamentals, which involve mostly the atomic displacements of the 2PY moiety of the dimer. The respective calculated frequencies are 559, 633, 842, 1261, and 1386 cm^{-1}, and the mode patterns are shown in Figure 2 of the Supporting Information. The corresponding measured monomer frequencies are 535, 601 806, 1228, and 1352 cm^{-1} (Figure 2b), and they have been assigned to benzenoid $6a_1^0$, $6b_1^0$, 1_1^0, 14_1^0, and 3_1^0 transitions, respectively. The correspondences between the monomer and dimer bands are indicated by dotted lines. The rest of the bands in the dimer spectrum can be interpreted as combinations of these fundamentals with the low-frequency intermolecular modes.

An interesting correlation between the vibrational frequencies of the monomer and dimer (Table 1) is that, except the C═O stretching, the other modes of 2PY···FA exhibit blue shifts in the range of 16−36 cm^{-1} compared to those of the bare 2PY molecule. The observed frequency of the C═O stretching fundamental of 2PY monomer is 1714 cm^{-1}, and in the dimer it is shifted to 1709 cm^{-1}. The corresponding calculated frequencies in the two cases are 1729 and 1683 cm^{-1}. The red shift of the C═O stretching vibration can easily be explained as due to partial decrease in bond order of this double bond on hydrogen bond formation. The possible explanation for the blue shifts observed for other modes of the dimer is due to enhanced resistance to molecular deformation by the two hydrogen bonds.

3.2. Theory. *3.2.A. Energetic and Geometric Parameters.* In a number of previous studies, quantum chemistry calculations at different levels of theory have been used for predictions of relative stability of the two tautomeric forms of the bare molecule as well as their hydrogen-bonded complexes with water in the gas phase.[29−35] 2HP has been predicted to be more stable than 2PY, but hydrogen-bonded complex formation with a solvent molecule shifts the tautomeric equilibrium toward 2PY. For example, a very recent calculation by Fu et al.[30] at the BH-LYP/6-311++G(2d,2p) level predicts that the energy difference between the two tautomers is 1.00 kcal/mol (in favor of 2HP) and the barrier for 2HP → 2PY conversion is 43.18 kcal/mol. The predictions are qualitatively comparable to what has been found experimentally. Thus, the abundance ratio of 2HP to 2PY in the gas phase at 356 K was estimated to be 3:1 using a microwave spectroscopic method.[28] A similar abundance ratio was also measured in inert gas matrixes using an IR spectroscopic method.[27]

The results of our calculations on the monomer at the DFT/B3LYP/6-311++G** level and at other levels (Table 2) agree with those of Fu et al.[30] and Barone et al.[31] The structure and energetic parameters 2HP···FA, 2PY···FA, and TS are calculated at the same level of theory. The optimized structures are shown in Figure 3, and the energetic parameters are shown schematically in Figure 4. The total energy of 2HP and FA

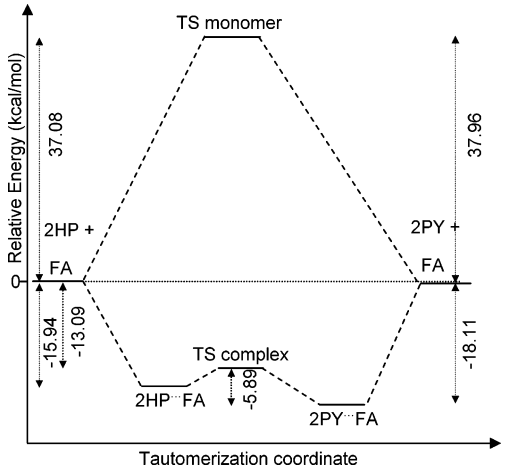

Figure 4. Energy-level diagram showing theoretically predicted relative energies of different molecular species and transition states. The total energy of 2HP and FA at infinite separation has been taken as zero (0) of the energy scale. The energy values (kcal/mol) shown are basis set superposition error (BSSE) uncorrected.

molecular pair at infinite separation is taken as the reference of the energy scale. A selection of the important geometric parameters of all the molecular species involved in the study are presented in Table 1 of the Supporting Information. The relative energies calculated at other levels of theory are also presented in the Supporting Information as Table 2.

Figure 4 shows that the formic acid assisted tautomerization barrier (zero point energy uncorrected) is remarkably smaller (by a factor of about 14) compared to that of the bare molecule. Recently we reported the DFT predictions of formamide to formamidic acid tautomerization and the catalytic role of formic acid in the process.[44] The energy barrier for the catalyzed process is predicted to be lowered by a factor of 4. For the 2HP ↔ 2PY system, Fu et al. have reported that, at the B3LYP/6-311++G-(2d,2p) level of calculation, the water assisted tautomerization barrier is predicted to be smaller by only a factor of 2.79. Similarly, at the MP2/6-31G** level of calculation,[35] the tautomerization barriers of 2HP(H_2O) and 2HP(H_2O)$_2$ complexes are lowered by only factors of 2.34 and 3.51, respectively. A comparison of these data with the results of the present study

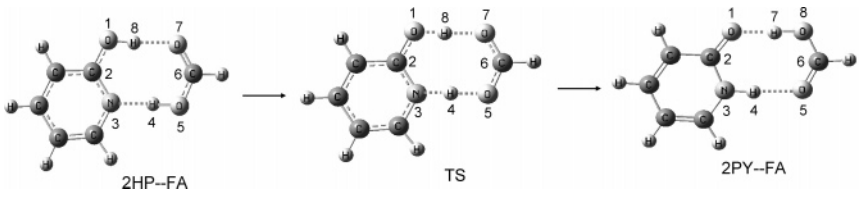

Figure 3. Optimized structures of 2HP···FA and 2PY···FA tautomers and the transition state species (TS) between the two forms.

TABLE 3: Energy Barriers (kcal/mol) for 2HP → 2PY and 2HP···FA → 2PY···FA Tautomeric Conversions Predicted by Different Levels of Calculation[a]

	2HP → 2PY		2HP···FA → 2PY···FA	
level of calculation	without ZPE[b] correction	ZPE corrected	without ZPE correction	ZPE corrected
MP2/6-31G**	37.46 (35.19)	34.37 (32.02)	5.08 (5.39)	2.07 (2.14)
B3LYP/6-31G**	35.39 (35.40)	32.32 (32.26)	2.53 (4.86)	−0.42 (1.62)
B3LYP/6-311++G**	37.08 (37.96)	33.89 (34.68)	2.85 (5.89)	−0.04 (2.71)

[a] The values in parentheses indicate the reverse reaction barrier height. [b] ZPE, zero-point energy.

TABLE 4: Differences in Geometric Parameters (ΔR) between the TS and Reactants, and Corresponding Energy Changes (ΔE, kcal/mol) Calculated at the B3LYP/6311++G Level Induced by Varying the Configurations of Isolated 2HP and the 2HP Moiety in 2HP···FA**

	2HP		2HP in 2HP···FA	
geometric parameters	ΔR	ΔE	ΔR	ΔE
O_1-H_8 (Å)	0.401	41.05	0.055	2.68
O_1-C_2 (Å)	−0.066	2.28	−0.027	0.73
C_2-N_3 (Å)	0.036	0.84	0.012	0.38
$-O_1-C_2-N_3$ (deg)	−12.1	7.67	0.7	0.11
$-C_2-O_1-H_8$ (deg)	−31.6	22.95	2.5	0.49

clearly indicates that formic acid is a very effective catalyst for 2HP ↔ 2PY tautomerization in the gas phase.

Table 3 shows that the barrier calculated at the MP2 level of theory is almost twice the DFT predicted barrier. Furthermore, in the latter method the predicted barrier turns out to be negative when zero point energy correction is incorporated. For the same correction, the MP2 predicted barrier is reduced from ∼5.0 to ∼2.0 kcal/mol. Overall, under the catalytic influence of formic acid, the tautomeric conversion turns out to be a nearly barrierless process, and this prediction appears to be consistent with our experimental results. It has been mentioned before that, in the experiment, the fluorescence signal of 2PY···FA appears to largely enhanced, but we could not detect any signal for the 2HP···FA species. A plausible explanation of this is that in the ground electronic state 2HP···FA is converted to 2PY···FA during collisional cooling in supersonic jet expansion. Such relaxation has been demonstrated earlier in many cases, particularly when the conversion barrier is low.[45] Of course, it is essential to mention that large enhancement of the fluorescence signal for 2PY···FA could also be due to its larger fluorescence quantum yield compared to bare 2PY. Likewise, the absence of the fluorescence signal of 2HP···FA could be due to its smaller fluorescence quantum yield compared to bare 2HP. However, such relative quantum yield values of fluorescence are not known. To verify this possibility for the case of 2HP···FA, we attempted to detect the species using the one-color resonance enhanced multiphoton ionization (REMPI) method. However, except for the cold and a few hot bands of the $S_1 \leftarrow S_0$ absorption system of bare 2HP, no new band was observed.

The origin of the catalytic influence of FA on the tautomeric conversion can be partly understood by examining the optimized structural parameters of various molecular and TS species, presented as Supporting Information (Table 1). It has been observed that the geometric parameters of the TS are fairly similar to those of the reactant (2HP···FA), but the values are quite off from those of the product (2PY···FA). Thus, the separations between O_1 and H_8 atoms in the reactant, TS, and product are 0.990, 1.045, and 1.588 Å, respectively. Such a correlation is also seen for separations between H_4 and O_5 atoms. The distortions of five important geometric parameters of 2HP and 2HP···FA that occur as a result of TS formation are presented in Table 4. The corresponding energy changes calculated by the configuration variation method at the B3LYP/6-311++G** level are also presented in the same table. The data indicate that the factors responsible for the smaller energy barrier of the catalytic process are the smaller distortions with respect to $-O_1-C_2-N_3$ and $-C_2-O_1-H_8$ bond angles and the O_1-H_8 bond length to reach the TS configuration. The two hydrogen bonds (involving N_3, H_4, O_5 and O_1, H_8, O_7 atoms) are mostly linear in reactant and TS, but partly distorted in the product. These similarities in geometric parameters of the TS with reactant are reflected in energetic parameters.

3.2.B. Potential Energy Surface. The potential energy surface for 2HP···FA → 2PY···FA conversion has been constructed by optimizing the geometries of the two complexes at the DFT/B3LYP/6-31G** level for discrete values of O_1-H_8 and H_4-O_5 bond lengths. The values of these two parameters were scanned from 0.9 to 2.0 Å at a step of 0.05 Å. The surface thus generated and the corresponding contour plot are presented in Figure 5. The two minima corresponding to the reactant and product, and the saddle point corresponding to the TS, are indicated in the figure. The identification of the TS configuration was subjected to IRC calculation, and the energy profile as a function of the reaction coordinate is shown in Figure 6. The normal-mode frequencies corresponding to the geometries of the reactant, TS, and product on the surface have been calculated at the DFT level using 6-31G** basis set. The vibrational mode of the TS for which the calculated frequency appears to be negative is identified as the reaction coordinate.

In Figure 7 we have presented how the three key internal coordinates, O_1-H_8, H_4-O_5, and C_2-C_6, evolve as a function of the intrinsic reaction coordinate. The configuration of the TS has been corresponded to the origin of the coordinate system. It indicates that the two hydrogen bond distances sharply increase for one unit of the reaction coordinate in the direction of the product (2PY···FA) from the TS configuration, but for the same change in the direction of the reactant the O−H distance remains practically unaltered. This happens because the structural parameters of the TS have more similarities with the reactant compared to the product. On the other hand, the distance between the C_2 and C_6 atoms remain practically the same within 0.7 unit of reaction coordinate in both the reactant and product directions.

The absence of any other minimum on the potential energy surface indicates that the most favorable mechanism of tautomerization in the ground electronic state is via a concerted hopping of the two protons. Sequential proton transfer would generate an ionic intermediate. The potential energy surface indicates that ionic configuration does not correspond to any

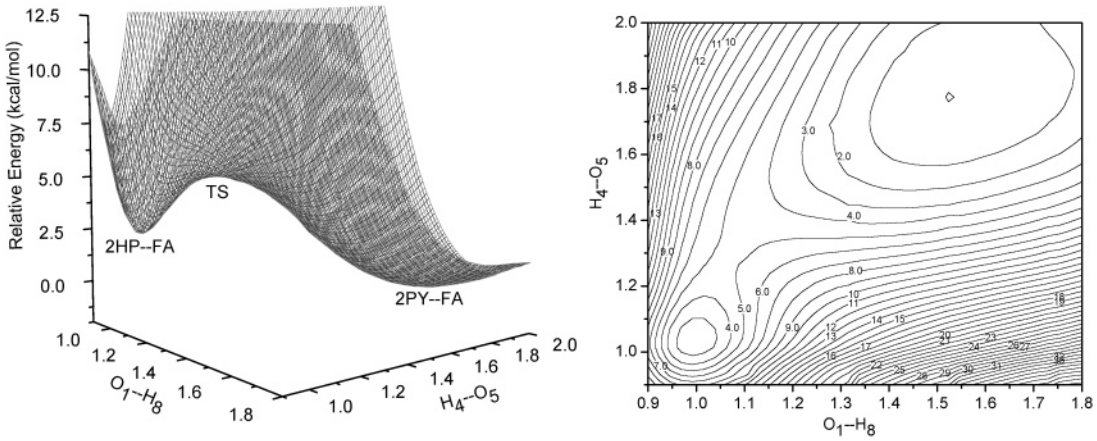

Figure 5. Potential energy surface and the corresponding contour plot as a function of O_1-H_8 and H_4-O_5 bond lengths.

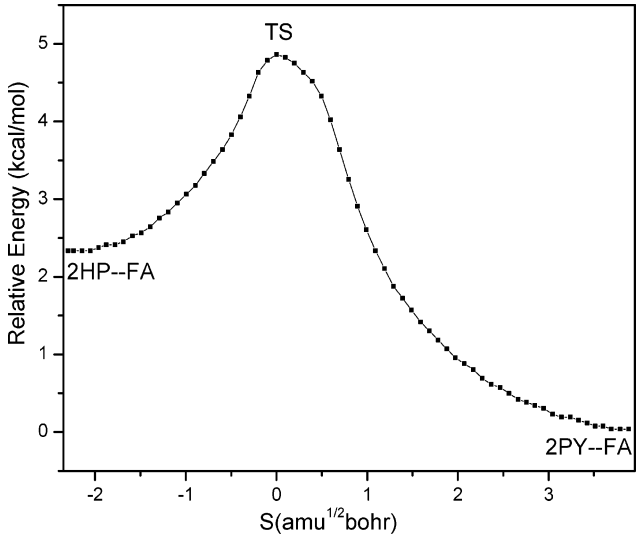

Figure 6. Energy profile of 2HP···FA → 2PY···FA tautomeric conversion as a function of intrinsic reaction coordinate (*S*).

distinct minimum. We have also searched for this possibility (i.e., ionic intermediate) by partially optimizing the ionic configurations using higher basis sets, but frequency calculations never support them to be local minima. A similar result is also observed in the case of water-assisted tautomerization.[34,35] A detailed knowledge of the mechanism of such processes in different systems is important for understanding the tautomerizations in DNA bases.

4. Summary

Laser-induced-fluorescence spectroscopy has been used with the aim of characterizing the doubly hydrogen bonded complexes of 2HP ↔ 2PY tautomeric pair with FA in the gas phase. However, in a supersonic jet expansion, only 2PY···FA complex has been identified, but the fluorescence as well as REMPI signals of the corresponding tautomeric complex (2HP···FA) is absent. Our theoretical predictions are consistent with the earlier predictions that 2HP is slightly more stable than 2PY, but the order of stability is reversed on complex formation with formic acid. The DFT/B3LYP/6-311++G** level calculated energy barrier for 2HP → 2PY conversion is ∼34 kcal/mol, whereas in the hydrogen-bonded complex the tautomeric conversion turns out to be a nearly barrierless process. The dispersed fluorescence spectra measured following excitations of the origin bands of 2PY monomer and 2PY···FA complex have been fully assigned with the aid of their theoretically

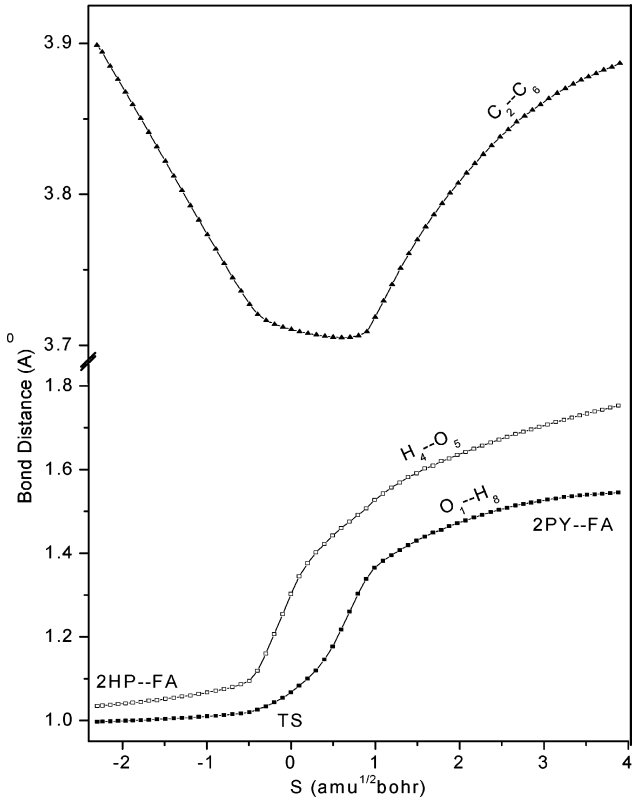

Figure 7. Evolution of the three key geometric parameters for 2HP···FA → 2PY···FA tautomeric conversion as a function of intrinsic reaction coordinate (*S*).

predicted normal-mode frequencies. The results of the present study indicate that an apparently unfavorable tautomeric conversion in a molecule can become facile if the molecule forms a multiply hydrogen bonded complex with a species having a simultaneous proton donor−acceptor property.

Acknowledgment. The financial support to carry out this research was received from the Department of Science and Technology, New Delhi, Government of India. M.K.H thanks the CSIR for a Senior Research Fellowship.

Supporting Information Available: Tables with bond angles and lengths of all molecular species at the DFT/B3LYP/6-311++G** level of theory and basis set superposition error (BSSE) corrected binding energies of 2-HP···FA and 2-PY···FA. Figures giving normal modes of the six intermolecular vibrations of the 2-PY···FA mixed dimer and normal modes

corresponding to assignments of the six vibronic bands in the dispersed fluorescence spectrum of 2-PY···FA. This material is available free of charge via the Internet at http://pubs.acs.org.

References and Notes

(1) Pullman, B.; Pullman, A. *Quantum Biochemistry*; Wiley-Interscience: New York, 1963.
(2) Löwdin, P. O. *Rev. Mod. Phys.* **1963**, *35*, 724.
(3) Bell, R. P. *The Proton in Chemistry*; Cornell University Press: Ithaca, NY, 1973.
(4) Florián, J.; Hrouda, V.; Hobza, P. *J. Am. Chem. Soc.* **1994**, *116*, 1457.
(5) Colominas, C.; Luque, F. J.; Orozco, M. *J. Am. Chem. Soc.* **1996**, *118*, 6811.
(6) Kryachko, E. S.; Sabin, J. R. *Int. J. Quantum Chem.* **2003**, *91*, 695.
(7) Gorb, L.; Podolyan, Y.; Dziekonski, P.; Sokalski, A.; Leszczynski, J. *J. Am. Chem. Soc.* **2004**, *126*, 10119.
(8) Frey, J. A.; Müller, A.; Frey, H.; Leutwyler, S. *J. Chem. Phys.* **2004**, *121*, 8237.
(9) Müller, A.; Losada, M.; Leutwyler, S. *J. Phys. Chem. A* **2004**, *108*, 157.
(10) Müller, A.; Leutwyler, S. *J. Phys. Chem. A* **2004**, *108*, 6156.
(11) Meuwly, M.; Müller, A.; Leutwyler, S. *Phys. Chem. Chem. Phys.* **2003**, *5*, 2663.
(12) Tautermann, C. S.; Voegele, A. F.; Liedl, K. R. *Chem. Phys.* **2003**, *292*, 47.
(13) Müller, A.; Talbot, F.; Leutwyler, S. *J. Am. Chem. Soc.* **2002**, *124*, 14486.
(14) Müller, A.; Talbot, F.; Leutwyler, S. *J. Chem. Phys.* **2002**, *116*, 2836.
(15) Müller, A.; Talbot, F.; Leutwyler, S. *J. Chem. Phys.* **2001**, *115*, 5192.
(16) Müller, A.; Talbot, F.; Leutwyler, S. *J. Chem. Phys.* **2000**, *112*, 3717.
(17) Borst, D. R.; Roscioli, J. R.; Pratt, D. W.; Florio, G. M.; Zwier, T. S.; Müller, A.; Leutwyler, S. *Chem. Phys.* **2002**, *283*, 341.
(18) Held, A.; Pratt, D. W. *J. Chem. Phys.* **1992**, *96*, 4869.
(19) Held, A.; Pratt, D. W. *J. Am. Chem. Soc.* **1990**, *112*, 8629.
(20) Schlegel, H. B.; Gund, P.; Fluder, E. M. *J. Am. Chem. Soc.* **1982**, *104*, 5347.
(21) Scanlan, M. J.; Hillier, I. *Chem. Phys. Lett.* **1984**, *107*, 330.
(22) Wong, M. W.; Wiberg, K. B.; Frisch, M. J. *J. Am. Chem. Soc.* **1992**, *114*, 1645.
(23) Ishikawa, H.; Iwata, K.; Hamaguchi, H. *J. Phys. Chem. A* **2002**, *106*, 2305.
(24) Hung, F.-T.; Hu, W.-P.; Li, T.-H.; Cheng, C.-C.; Chou, P.-T. *J. Phys. Chem. A* **2003**, *107*, 3244.
(25) Beak, P.; Fry, F. S. *J. Am. Chem. Soc.* **1973**, *95*, 1700.
(26) Nimlos, M. R.; Kelley, D. F.; Bernstein, E. R. *J. Phys. Chem.* **1989**, *93*, 643.
(27) Nowak, M. J.; Lapinski, L.; Fulara, J.; Les, A.; Adamowicz, L. *J. Phys. Chem.* **1992**, *96*, 1562.
(28) Hattherley, L. D.; Brown, R. D.; Godfrey, P. D.; Pierlot, A. P.; Caminati, W.; Damiani, D.; Melandri, S.; Favero, L. B. *J. Phys. Chem.* **1993**, *97*, 46.
(29) Inuzuka, K. *J. Chem. Soc. Jpn. (Nippon Kagaku Kaishi)* **1999**, No. 8, 509.
(30) Fu, A.; Li, H.; Du, D.; Zhou, Z. *J. Phys. Chem. A* **2005**, *109*, 1468.
(31) Barone, V.; Adamo, C. *J. Phys. Chem.* **1995**, *99*, 15062.
(32) Moreno, M.; Miller, W. H. *Chem. Phys. Lett.* **1990**, *171*, 475.
(33) Chou, P. T.; Wei, C. Y. *J. Phys. Chem. B* **1997**, *101*, 9119.
(34) Tsuchida, N.; Yamabe, S. *J. Phys. Chem. A* **2005**, *109*, 1974.
(35) Li, Q.; Fang, W.; Yu, J. *J. Phys. Chem. A* **2005**, *109*, 3983.
(36) Das, A.; Mahato, K. K.; Chakraborty, T. *J. Chem. Phys.* **2001**, *114*, 6107.
(37) Frisch, M. J.; Trucks, G. W.; Schlegel, H. B.; et al. *Gaussian 03*, revision B.05; Gaussian Inc.: Pittsburgh, PA, 2003.
(38) Peng, C.; Ayala, P. Y.; Schlegel, H. B.; Frisch, M. J. *J. Comput. Chem.* **1996**, *17*, 49.
(39) Boys, S. F.; Bernardi, F. *Mol. Phys.* **1970**, *19*, 553.
(40) Matsuda, Y.; Ebata, T.; Mikami, N. *J. Chem. Phys.* **1999**, *110*, 8397.
(41) Matsuda, Y.; Ebata, T.; Mikami, N. *J. Chem. Phys.* **2000**, *113*, 573.
(42) Matsuda, Y.; Ebata, T.; Mikami, N. *J. Phys. Chem. A* **2001**, *105*, 3475.
(43) Varsanyi, G. *Vibrational spectra of Benzene Derivatives*; Academic: New York, 1969.
(44) Hazra, M. K.; Chakraborty, T. *J. Phys. Chem. A* **2005**, *109*, 7621.
(45) Ruoff, R. S.; Klots, T. D.; Emilsson, T.; Gutowsky, H. S. *J. Chem. Phys.* **1990**, *93*, 3142.